Supplemental material

Kriebel et al., https://doi.org/10.1083/jcb.201710170

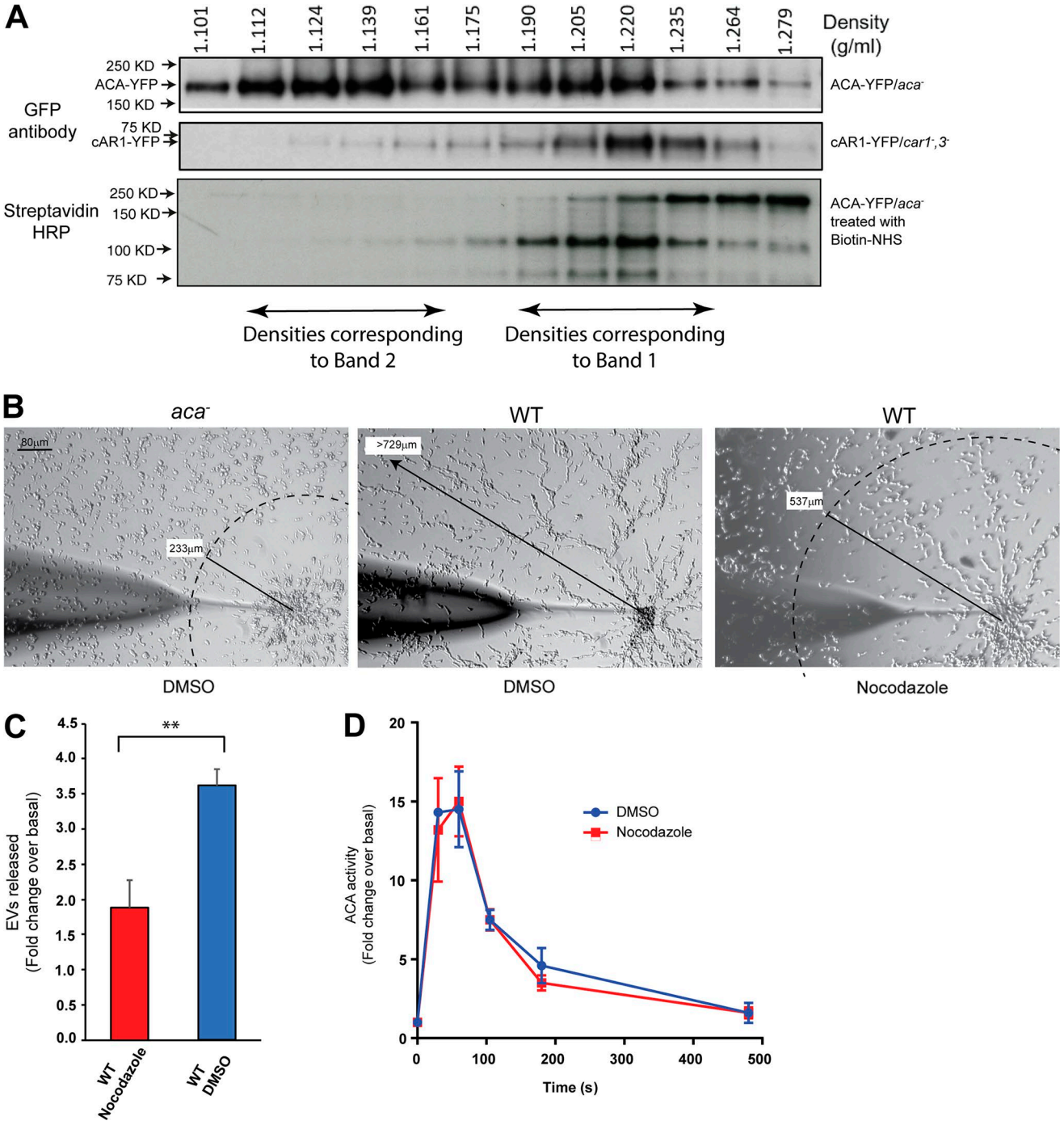

Figure S1. **Assessment of purity and effects of nocodazole on vesicle release and cell migration. (A)** Immunoblot analysis of sucrose density fractions of extracts derived from ACA-YFP/*aca*⁻, cAR1-YFP/*cAR1/3*$^{-/-}$, and surface biotinylated ACA-YFP/*aca*⁻ cells. YFP was detected using an antibody specific for GFP, and biotin was detected with HRP-conjugated streptavidin. **(B)** Micropipette streaming assays of WT cell treated with either DMSO or 60 µM Noco. *aca*⁻ cells were used as signal relay negative controls (left). Images were taken 15 min after placing a micropipette filled with 1 µM cAMP in a bed of cells pulsed for 5 h with cAMP. Arrows and broken lines show the extent of cell recruitment. **(C)** Nanoparticle tracking analysis of EVs released from WT cells treated with either DMSO or 60 µM Noco. Values normalized over residual basal amounts (see Materials and methods) are shown as the mean of three independent experiments, which in turn were derived from the mean of three technical replicates. **, $P < 0.002$; significance testing was performed using unpaired two-tailed *t* test assuming a Gaussian distribution. **(D)** Adenylyl cyclase activity in cell lysates derived from DMSO or Noco-treated cells after the addition of 1 µM cAMP. Results presented as mean ± SEM of three independent experiments.

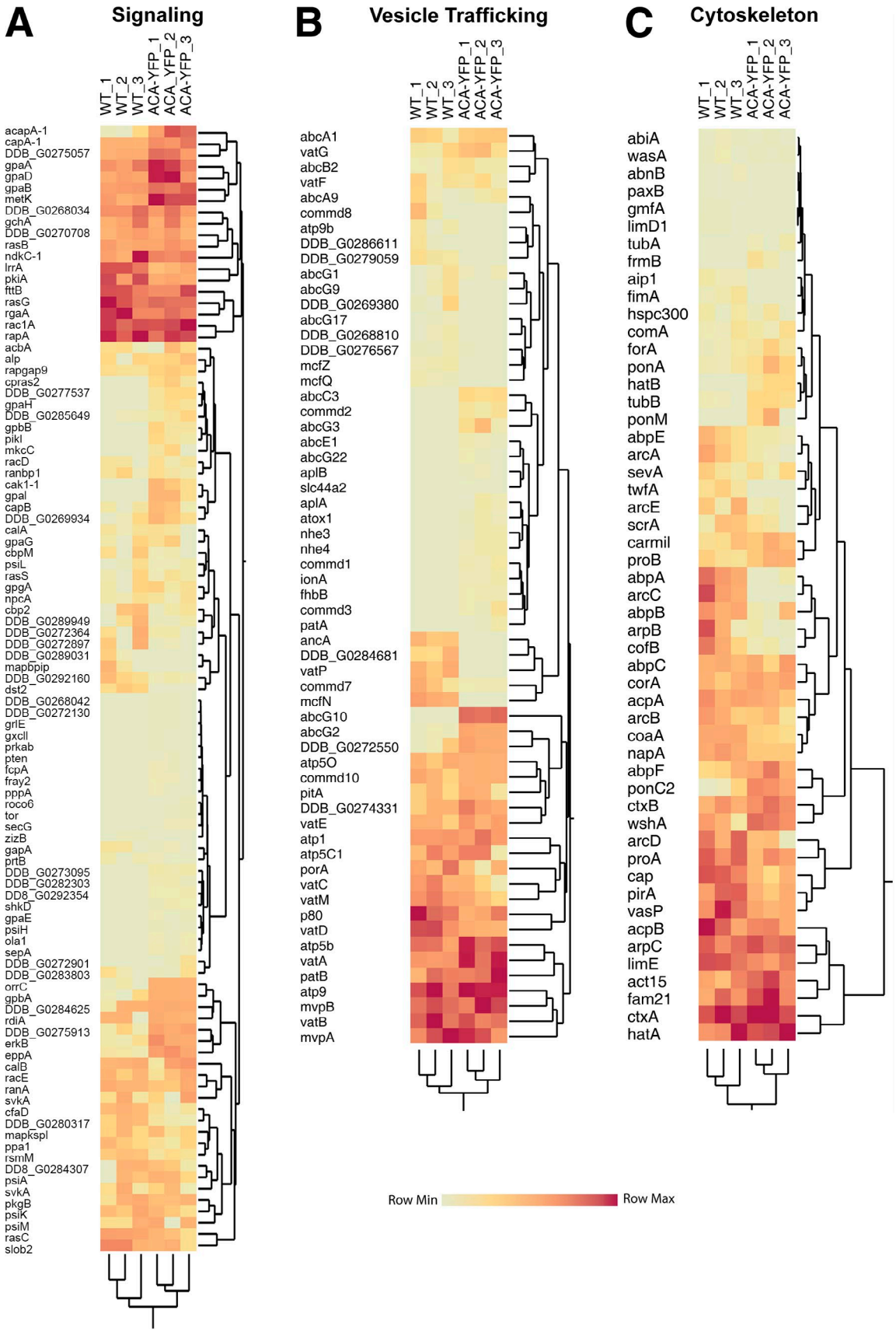

Figure S2. **Heat maps and cluster analyses of relative PSMs of proteins involved in signaling, vesicle trafficking, and cytoskeleton.** Data derived from three separate MS analysis for EVs derived from either ACA-YFP/*aca*⁻ or WT cells. Shaded colors in each map represent the relative PSMs in each column.

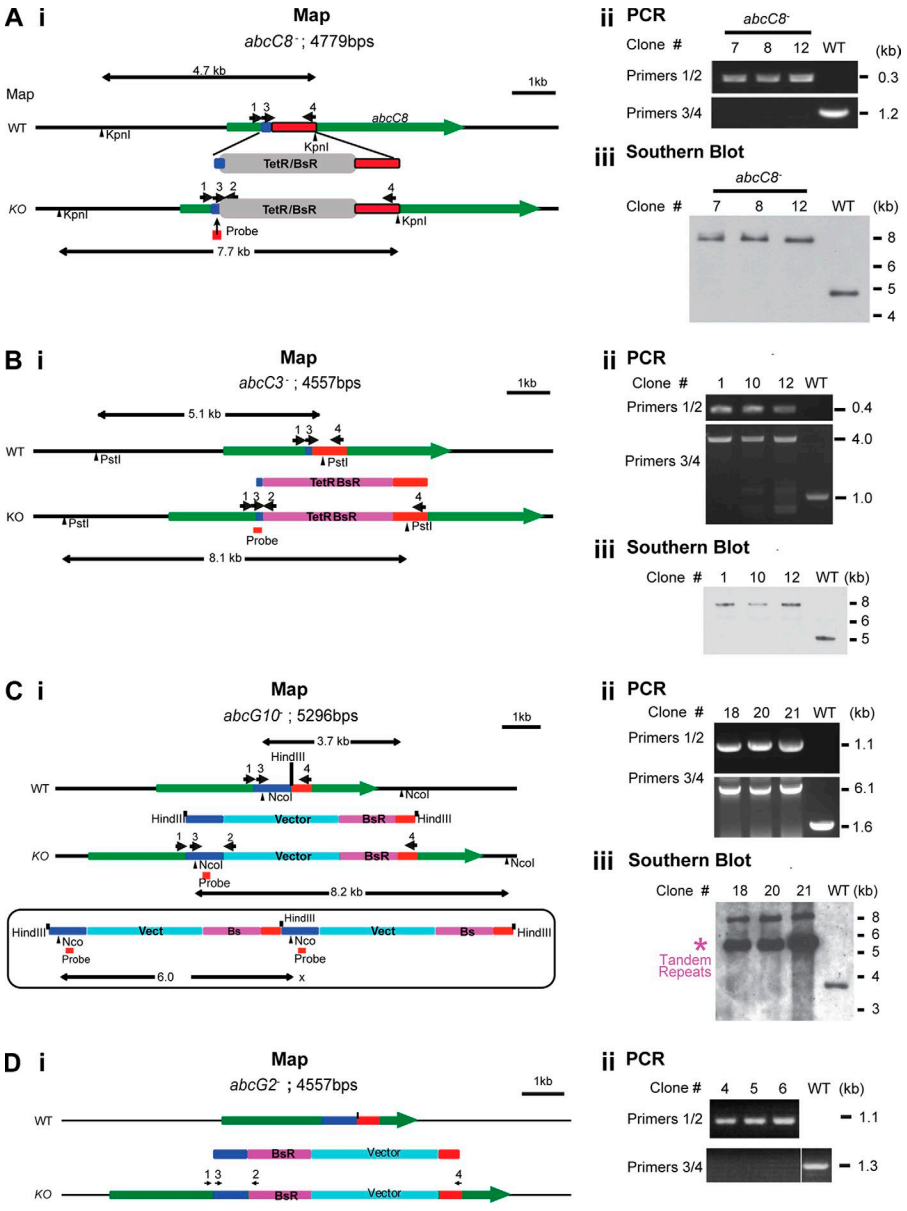

Figure S3. **Generation of *abcC3*, *abcC8*, *abcG10*, and *abcG2* knockout cell lines. (A [i])** Map of the knockout strategy for the *abcC8* gene by inserting the TetR/BsR cassette flanked by the appropriate *abcC8* flanking sequences (red and blue) to guide insertion. **(A [ii])** PCR confirmation of *abcC8*⁻ knockouts. All three clones were positive for a 0.3-kb band that includes the sequence joining *abcC8* and the TetR/BsR cassette and absent for the 1.2-kb band that includes the sequence from *abcC8* without the TetR/BsR cassette. **(A [iii])** Southern blot confirmation of *abcC8* knockouts. All three clones hybridized the 8-kb fragment labeled by the probe (red) and clipped by the Kpn1 restriction enzyme. All three clones did not hybridize the 4.7-kb fragment that excluded the TetR/BsR cassette. **(B [i])** Diagram depicting the knockout strategy for the *abcC3* gene. Exon 4 of the *abcC3* gene was disrupted by the insertion of a blasticidin resistance cassette (TetRBsR; magenta). Green represents the entire *abcC3* gene. Blue is the 5′ fragment, and red is the 3′ fragment of exon 4 used to orient the resistance cassette for recombination. **(B [ii])** PCR genomic analysis using primer sets 1/2 and 3/4. Primer set 1/2 amplified a 0.4-kb region in *abcC3*⁻ cells. Primer set 3/4 amplified a 4.0-kb region in WT cells and a 1.0-kb region in *abcC3*⁻ cells. **(B [iii])** Genomic DNA was digested with PstI and analyzed by Southern blotting with a DNA fragment corresponding to the region designated as the probe in Ai. After digestion, a 5.1-kb band was generated from WT cells, whereas an 8.1-kb band was generated from *abcC3*⁻ cells. **(C [i])** Diagram depicting the knockout strategy for the *abcG10* gene. Exon 6 of the *abcG10* gene was disrupted by the insertion of a vector (light blue) containing a blasticidin resistance cassette (BsR; magenta). Green represents the entire *abcG10* gene. Blue is the 5′ fragment, and red is the 3′ fragment in exon 6 used to orient the resistance cassette for recombination. **(C [ii])** PCR genomic analysis using primer sets 1/2 and 3/4. Primer set 1/2 amplified a 1.1-kb region in *abcG10*⁻ cells. Primer set 3/4 amplified a 1.6-kb region in WT cells and a 6.1-kb region in *abcG10*⁻ cells. **(C [iii])** Genomic DNA was digested with NcoI and analyzed by Southern blotting with a DNA fragment corresponding to the region designated as the probe in Ai. After digestion, a 3.7-kb band was generated from WT cells, whereas an 8.2-kb band was generated from *abcG10*⁻ cells. Asterisk indicates a 6.0-kb band in *abcG10*⁻ cells, which might represent a tandem repeat as shown in the box. **(D [i])** Diagram depicting the knockout strategy for the *abcG2* gene. Exon 3 of the *abcG2* gene was disrupted by the insertion of a vector (light blue) containing the blasticidin resistance cassette (BsR; magenta). Green represents the entire *abcG2* gene. Blue is the 5′ fragment, and red is the 3′ fragment of exon 3 used to orient the resistance cassette for recombination. **(D [ii])** PCR genomic analysis using primer sets 1/2 and 3/4. Primer set 1/2 amplified a 1.1-kb region in *abcG2*⁻ cells. Primer set 3/4 amplified a 1.3-kb region in WT cells.

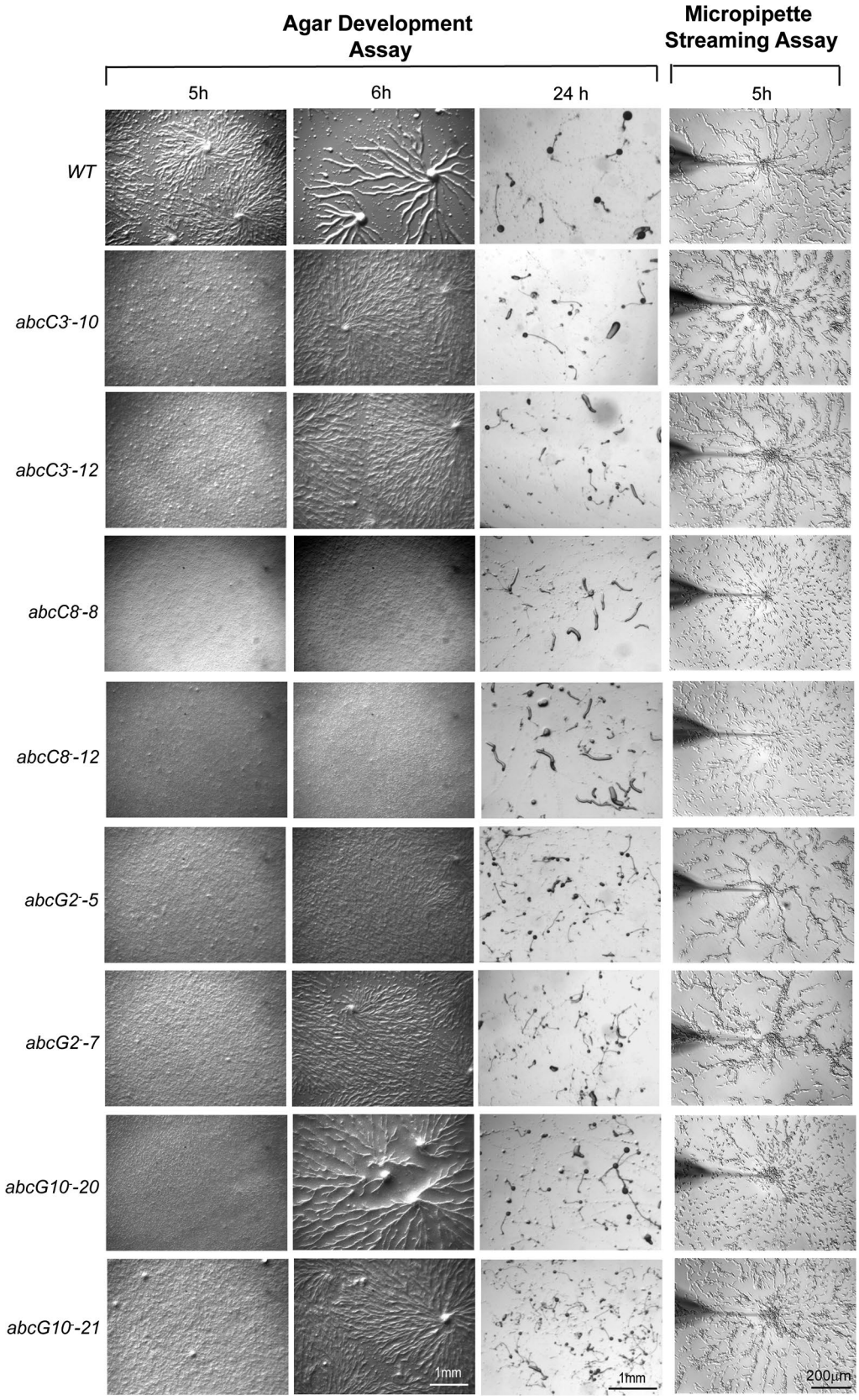

Figure S4. **Agar development and micropipette streaming assays of WT and ABC knockout mutants.** Left: Agar development assay of WT and ABC knockout mutant cell lines. Images of cells plated on top of agar taken 5, 6, and 24 h after cells were starved and plated at 10^6 per 10-mm plate. Right: Micropipette streaming assays of WT and ABC knockout mutants. Images were taken 15 min after placing a micropipette filled with 1 µM cAMP in a bed of cells pulsed for 5 h with cAMP. For both assays, two different clones of each knockout were evaluated.

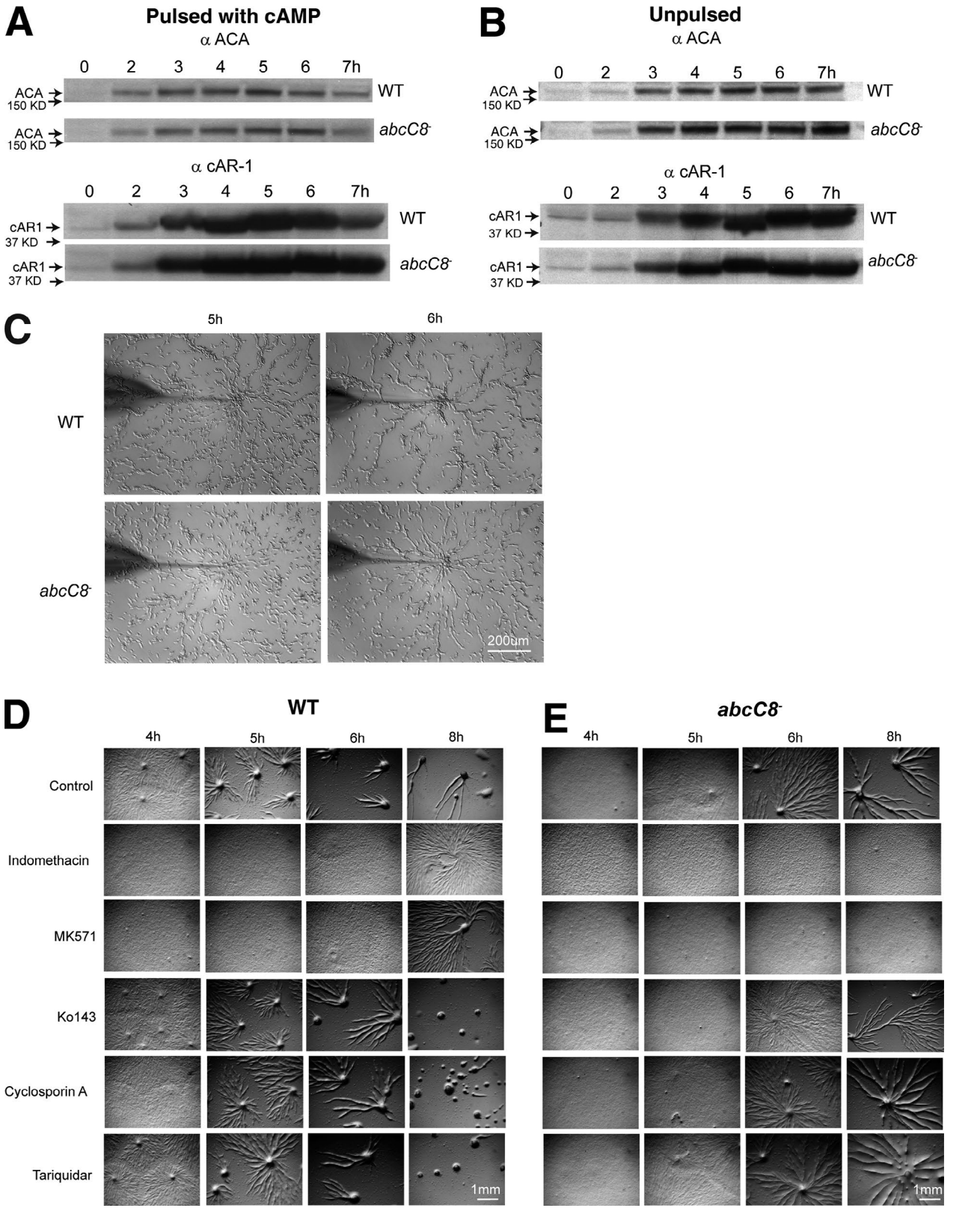

Figure S5. ***abcC8⁻* cells phenotypic characterization. (A and B)** Western blots of ACA and cAR1 from WT and *abcC8⁻* cells. WT and *abcC8⁻* cells were either not pulsed (A) or pulsed (B) with cAMP, and samples were taken at 1, 2, 3, 4, 5, 6, 7, and 8 h. Cell lysates were blotted with ACA and cAR1 antibodies. **(C)** *abcC8⁻* cells partly recover streaming in later development. Images of WT and *abcC8⁻* cells migrating toward a micropipette filled with 1 µM cAMP. Cells were pulsed for 5 or 6 h with cAMP. **(D and E)** ABCC class inhibitors inhibit streaming. Images depicting the response of WT (D) and *abcC8⁻* (E) cells developing on DB agar in the presence or absence of ABC transporter inhibitors. Images were taken at 4, 5, 6, and 8 h after development. DMSO (control), indomethacin, MK571, Ko143, cyclosporine A, and tariquidar were mixed into the agar at the concentrations indicated and added to cells when plated on the DB agar plates.

Video 1. **Ultrastructural imaging of vesicle release from chemotaxing *D. discoideum* cells. (A)** Serial longitudinal FIB-SEM images of the vesicle release and trail formation as indicated by the blue box in Fig. 1 A (ii). **(B)** Serial longitudinal FIB-SEM images taken of the two cells in Fig. 1 A (i) stained with colloidal gold (white) migrating toward a cell aggregate (shown at 15-nm slice/frame per second [fps]).

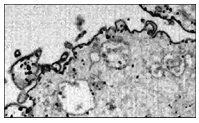

Video 2. **Serial longitudinal FIB-SEM images of a cell section showing intact and PM-fused MVB containing ACA-positive intralumenal vesicle.**

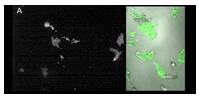

Video 3. **Vesicular trails released by migrating cells are capable of attracting other cells. (A and B)** Epifluorescent videos of ACAYFP/*aca*⁻ cells moving toward a spontaneously formed aggregate of cells. B also features an overlay of fluorescent and bright-field frames of ACAYFP/*aca*⁻ cells. Images were taken every 7 s and are shown at 10 fps.

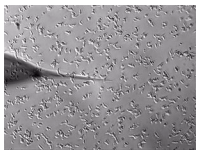

Video 4. **Control video showing migratory behavior of WT cells to a micropipette filled with buffer.**

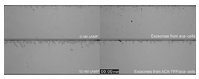

Video 5. **EZ-TAXIScan videos of *aca*⁻ cells migrating toward buffer, 10 nM cAMP, or EVs derived from either ACAYFP/*aca*⁻ or *aca*⁻ cells.** Images were taken every 15 s and are shown at 30 fps.

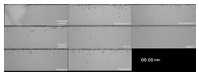

Video 6. **EZ-TAXIScan movies of *aca*⁻ cells migrating toward EVs derived from ACAYFP/*aca*⁻ cells treated with DMSO (control), indomethacin, MK571, Ko143, cyclosporine A, or tariquidar.** See Table S3 for concentration of inhibitors used. Images were taken every 15 s and are shown at 30 fps.

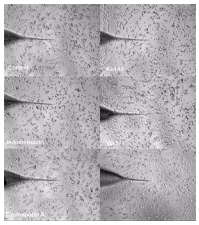

Video 7. **Videos of WT cells migrating toward a micropipette filled with 1 µM cAMP.** The cells were treated with DMSO (control), indomethacin, MK571, Ko143, cyclosporine A, and tariquidar. Images were taken every 10 s and are shown at 20 fps.

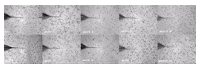

Video 8. **Video of WT, *abcC3*⁻, *abcC8*⁻, *abcG2*⁻, or *abcg10*⁻ cells migrating toward a micropipette filled with 1 µM cAMP.** Two clones of each cell type are shown. Images were taken every 10 s and are shown at 20 fps.

Table S1 is a comprehensive listing of all proteins identified in EVs derived from either WT or ACA-YFP/aca⁻ cells.

Table S2. **List of ABC transporters identified in exosomes**

Gene ID	Gene symbol	WT total PSM	ACA-YFP/*aca*⁻ total PSM
DDB_G0291994	abcA1	36	ND
DDB_G0291980	abcA9	19	ND
DDB_G0293438	abcB2	17	38
DDB_G0287691	abcC3	8	57
DDB_G0284867	abcC8	ND	3
DDB_G0290483	abcE1	ND	17
DDB_G0269214	abcG1	11	10
DDB_G0275689	abcG2	25	164
DDB_G0287461	abcG3	4	66
DDB_G0293450	abcG9	13	ND
DDB_G0292986	abcG10	9	380
DDB_G0273073	abcG17-1	28	10
DDB_G0270826	abcG22	16	11

ND, not detected.

Table S3. **List of ABC transporter inhibitors used in experiments, with representative reported inhibitory activity against each transporter class**

ABC inhibitor	ABCB1, (P-gp) IC50	ABCG2 (BCRP) IC50	ABCC (MRPs) IC50	Concentration used
Tariquidar	5 nM (Kannan et al., 2011)	100 nM (Kannan et al., 2011)	No inhibition (Kannan et al., 2011)	4 µM
Cyclosporine A	1 µM (Qadir et al., 2005)	50 µM (Bakhsheshian et al., 2013)	>50 µM (Wortelboer et al., 2005)	50 µM
Verapamil	5 µM (Tsuruo et al., 1981)	>100 µM (Henrich et al., 2006)	>100 µM (Klokouzas et al., 2001)	100 µM
Ko143	>100 µM (Weidner et al., 2015)	100 nM (Weidner et al., 2015)	20 µM (Weidner et al., 2015)	4 µM
MK571	No inhibition (Gekeler et al., 1995)	No inhibition (Mahringer et al., 2009)	5 µM (Gekeler et al., 1995)	50 µM
Indomethacin	No inhibition (Draper et al., 1997)	No inhibition (Elahian et al., 2010)	50 µM (El-Sheikh et al., 2007)	200 µM

Table S4. **Primers used for genotyping knockout mutant**

Name	Sequence (5′–3′)	Position on genomic sequence
abcC3-1	GCCTATGTTCCACAACAAGCATG	1,831–1,853
abcC3-2 (TetR AS2)	GAGCGCATTGTTAGATTTCATACAC	
abcC3-3	TCTCCGCGGTTCACCATATGACGT	1,890–1,906
abcC3-4	CGACCGCGGTAAAGAATACCAA	2,922–2,908
abcC8-1	GAGATTTCAAAAGAAGTTAATGCC	671–694
abcC8-2 (TetR AS2)	GAGCGCATTGTTAGATTTCATACAC	
abcC8-3	AGACCGCGGATGTACCAACATTGG	771–788
abcC8-4	GAGCCGCGGTACCCTTGGTT	2,018–2,005
abcG2-1	GGATTCCAAAGTTGATATCAAAGC	2,270–2,292
abcG2-2 (Act15p)	CCAACCCAAGTTTTTTTAAACC	
abcG2-3	AACCGCGGGTATGTTACTTGCTTTAAT	2,438–2,458
abcG2-4	TTCCGCGGTTGGAAGTACAGTTG	3,780–3,763
abcG10-1	GTATCGTCCATCAGCACTTCATATTGC	2,376–2,402
abcG10-2 (M13F)	GTAAAACGACGGCCAG	
abcG10-3	ATCCGCGGTTTACAAGTTGATGCAGGT	2,476–2,496
abcG10-4	ATCCGCGGATGAAATTTGAACAGTTGCA	4,090–4,068

References

Bakhsheshian, J., M.D. Hall, R.W. Robey, M.A. Herrmann, J.Q. Chen, S.E. Bates, and M.M. Gottesman. 2013. Overlapping substrate and inhibitor specificity of human and murine ABCG2. *Drug Metab. Dispos.* 41:1805–1812.

Draper, M.P., R.L. Martell, and S.B. Levy. 1997. Indomethacin-mediated reversal of multidrug resistance and drug efflux in human and murine cell lines overexpressing MRP, but not P-glycoprotein. *Br. J. Cancer.* 75:810–815.

Elahian, F., F. Kalalinia, and J. Behravan. 2010. Evaluation of indomethacin and dexamethasone effects on BCRP-mediated drug resistance in MCF-7 parental and resistant cell lines. *Drug Chem. Toxicol.* 33:113–119.

El-Sheikh, A.A., J.J. van den Heuvel, J.B. Koenderink, and F.G. Russel. 2007. Interaction of nonsteroidal anti-inflammatory drugs with multidrug resistance protein (MRP) 2/ABCC2- and MRP4/ABCC4-mediated methotrexate transport. *J. Pharmacol. Exp. Ther.* 320:229–235.

Gekeler, V., W. Ise, K.H. Sanders, W.R. Ulrich, and J. Beck. 1995. The leukotriene LTD4 receptor antagonist MK571 specifically modulates MRP associated multidrug resistance. *Biochem. Biophys. Res. Commun.* 208:345–352.

Henrich, C.J., H.R. Bokesch, M. Dean, S.E. Bates, R.W. Robey, E.I. Goncharova, J.A. Wilson, and J.B. McMahon. 2006. A high-throughput cell-based assay for inhibitors of ABCG2 activity. *J. Biomol. Screen.* 11:176–183.

Kannan, P., S. Telu, S. Shukla, S.V. Ambudkar, V.W. Pike, C. Halldin, M.M. Gottesman, R.B. Innis, and M.D. Hall. 2011. The "specific" P-glycoprotein inhibitor Tariquidar is also a substrate and an inhibitor for breast cancer resistance protein (BCRP/ABCG2). *ACS Chem. Neurosci.* 2:82–89.

Klokouzas, A., M.A. Barrand, and S.B. Hladky. 2001. Effects of clotrimazole on transport mediated by multidrug resistance associated protein 1 (MRP1) in human erythrocytes and tumour cells. *Eur. J. Biochem.* 268:6569–6577.

Mahringer, A., J. Delzer, and G. Fricker. 2009. A fluorescence-based in vitro assay for drug interactions with breast cancer resistance protein (BCRP, ABCG2). *Eur. J. Pharm. Biopharm.* 72:605–613.

Qadir, M., K.L. O'Loughlin, S.M. Fricke, N.A. Williamson, W.R. Greco, H. Minderman, and M.R. Baer. 2005. Cyclosporin A is a broad-spectrum multidrug resistance modulator. *Clin. Cancer Res.* 11:2320–2326.

Tsuruo, T., H. Iida, S. Tsukagoshi, and Y. Sakurai. 1981. Overcoming of vincristine resistance in P388 leukemia in vivo and in vitro through enhanced cytotoxicity of vincristine and vinblastine by verapamil. *Cancer Res.* 41:1967–1972.

Weidner, L.D., S.S. Zoghbi, S. Lu, S. Shukla, S.V. Ambudkar, V.W. Pike, J. Mulder, M.M. Gottesman, R.B. Innis, and M.D. Hall. 2015. The inhibitor Ko143 is not specific for ABCG2. *J. Pharmacol. Exp. Ther.* 354:384–393.

Wortelboer, H.M., M. Usta, J.J. van Zanden, P.J. van Bladeren, I.M. Rietjens, and N.H. Cnubben. 2005. Inhibition of multidrug resistance proteins MRP1 and MRP2 by a series of alpha,beta-unsaturated carbonyl compounds. *Biochem. Pharmacol.* 69:1879–1890.